Turkish Journal of Electrical Engineering & Computer Sciences

http://journals.tubitak.gov.tr/elektrik/

Research Article

Turk J Elec Eng & Comp Sci
(2013) 21: 2205 – 2217

doi:10.3906/elk-1203-128

A low-voltage and low-power sinh-domain universal biquadratic filter for low-frequency applications

Farooq KHANDAY,* **Nisar SHAH**
Department of Electronics and Instrumentation Technology, University of Kashmir, Srinagar, India

Received: 29.03.2012 • **Accepted:** 01.08.2012 • **Published Online:** 30.10.2013 • **Printed:** 25.11.2013

Abstract: Sinh-domain CMOS filters have favorable properties, such as a wide dynamic range at low supply voltage, compactness, linearity, and low power consumption. These properties are becoming increasingly important for biomedical applications that require extremely low-power dissipation and neuromorphic circuits that attempt to reproduce the biophysics of biological neurons and synapses. In this paper, a low-voltage sinh-domain universal biquadratic filter circuit is introduced. The circuit, aside from permitting the independent adjustment of pole frequency (ω_0) and the quality factor (Q), is free from matching conditions, capable of absorbing the shunt parasitic capacitances, amenable for monolithic integration, and composed of merely a few transconductor cells and grounded elements. The other features of the circuit are its low sensitivity and good linearity. Simulated results are obtained to prove the theoretical analyses and the filter shows a dynamic range of 59.17 dB and power consumption of only 19.2 nW.

Key words: Continuous-time filters, analog filters, companding filters, sinh-domain filters, biomedical electronics

1. Introduction

Since the early 1990s, there has been growing interest in the current-mode design approach [1]. Current-mode circuits have been shown to have a wide variety of useful features, including the capability of operating with a large bandwidth at low supply voltages [2]. Companding filters are an interesting subclass of current-mode analog filters, with the potential for low-voltage operation and electronic tuning capabilities [3,4]. The main concept of the companding filtering is the following: the linear input current is initially converted to a nonlinear compressed voltage and, as a next step, is processed by a companding core. The resulting compressed output voltage is then expanded and simultaneously converted into a linear current. In sinh-domain filtering, the compression of the input current could be performed by the inverse of the hyperbolic sine function, realized by translinear loops formed by bipolar transistors in an active region or metal-oxide semiconductor (MOS) transistors in a weak inversion [5–8].

Human biological signals operate in subhertz to several kilohertz, with amplitude in the range of microvolts [9]. To record these types of signals, complex, high-performance, and low-noise analog preprocessing blocks, preamplifiers, and filters are employed. In addition, these circuits should not introduce any form of distortion that can destroy the information contained over the frequency of interest [10]. Sinh filters are inherently class-AB [11–13] and, as such, possess the potential for a high dynamic range and possible biomedical applications (e.g., electroencephalography (EEG) or ultrasound, [9,14]). In applications with low frequency and

*Correspondence: farooqsnn20@yahoo.co.in

large number of filter stages, where the relative increase in power does not compromise the overall system's power budget, the sinh paradigm might have a comparative advantage in terms of minimizing the chip area cost [15].

An important subclass of second-order filters is the universal biquadratic filters, denoted as the topologies, which offer the 5 standard filter functions: low-pass (LP), high-pass (HP), band-pass (BP), band-stop (BS), and all-pass (AP). Universal biquadratic filters are widely used in the realization of analog signal processing systems, such as 3-way crossover networks for high-fidelity loudspeakers, touchtone telephone systems, and phase-locked loop FM stereo demodulators [16]. According to the authors' best knowledge, sinh-domain universal biquadratic filters have not yet been introduced in the literature.

Thus, a low-voltage sinh-domain universal biquadratic filter circuit that has the advantages of a tunable cut-off frequency, wide dynamic range, and low power consumption is introduced in this paper. The proposed circuit's low-power and compactness features, combined with its capabilities of generating low cut-off frequencies, make it ideal for biomedical applications [17,18], as well as neuromorphic systems that require large filter bank arrays, such as silicon cochleae or pulse-based neural network devices [19,20]. In addition, the resonant frequency (ω_0) and Q factor of the filters could be independently adjusted, offering design flexibility.

The paper is organized as follows: the sinh-domain universal biquadratic filter is introduced in Section 2. Sinh-domain building blocks are presented in Section 3. In order to confirm the validity of the design, the sinh-domain universal biquadratic filter has been realized in Section 4. The performance of the derived topology has been evaluated through simulation results, where the most important performance factors have been taken into account.

2. Design procedure of the sinh-domain universal biquadratic filter

The derivation of the proposed universal biquadratic filter has been achieved by employing the following set of complementary SINH^{-1} and SINH operators [15], which are described by Eqs. (1) and (2) as:

$$\hat{v}_{IN} = SINH^{-1}(i_{in}) = U_T.\sinh^{-1}\left(\frac{i_{in}}{2I_o}\right), \tag{1}$$

$$i_{out} \equiv SINH(\hat{v}_{OUT}) = 2I_o.\sinh\left(\frac{\hat{v}_{OUT}}{U_T}\right), \tag{2}$$

where $U_T = nV_T$, n is the subthreshold slope factor of a MOS transistor in a weak inversion, and V_T is the well-known thermal voltage.

The functional block diagram (FBD) of the proposed sinh-domain universal biquadratic filter is demonstrated in Figure 1, where the realized transfer functions are described by Eqs. (3)–(7):

$$H_{HP}(s) = \frac{SINH(\hat{v}_{HP})}{SINH(\hat{v}_{IN})} = \frac{s^2}{s^2 + \frac{K}{\hat{\tau}_1}s + \omega_0^2}, \tag{3}$$

$$H_{LP}(s) = \frac{SINH(\hat{v}_{LP})}{SINH(\hat{v}_{IN})} = \frac{\omega_0^2}{s^2 + \frac{K}{\hat{\tau}_1}s + \omega_0^2}, \tag{4}$$

$$H_{BP}(s) = \frac{SINH(\hat{v}_{BP})}{SINH(\hat{v}_{IN})} = \frac{\frac{K}{\hat{\tau}_1}s}{s^2 + \frac{K}{\hat{\tau}_1}s + \omega_0^2}, \tag{5}$$

$$H_{BR}(s) = \frac{SINH(\hat{v}_{BR})}{SINH(\hat{v}_{IN})} = \frac{s^2 + \omega_0^2}{s^2 + \frac{K}{\hat{\tau}_1}s + \omega_0^2}, \tag{6}$$

$$H_{AP}(s) = \frac{SINH(\hat{v}_{AP})}{SINH(\hat{v}_{IN})} = \frac{s^2 - \frac{K}{\hat{\tau}_1}s + \omega_0^2}{s^2 + \frac{K}{\hat{\tau}_1}s + \omega_0^2}, \tag{7}$$

where the variable K denotes a scaling factor.

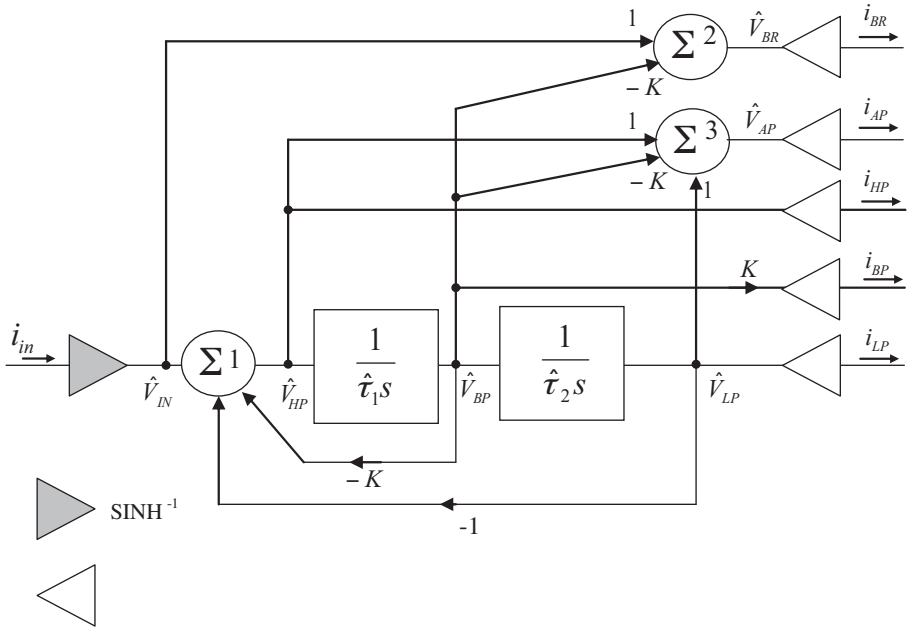

Figure 1. FBD of the proposed sinh-domain universal biquadratic filter.

The resonant frequency (ω_0) and the Q factor of the filter are given by Eqs. (8) and (9) as:

$$\omega_0 = \frac{1}{\sqrt{\hat{\tau}_1.\hat{\tau}_2}}, \tag{8}$$

$$Q = \frac{1}{K}.\sqrt{\frac{\hat{\tau}_1}{\hat{\tau}_2}}. \tag{9}$$

After examining Eqs. (8) and (9), it is clear that the resonant frequency (ω_0) and Q factor of the filters could be independently adjusted by the scale factor K.

The circumflex ($\wedge$) in the time constants of the integrators indicates that they are in the sinh-domain. From Figure 1, it is clear that to realize the sinh-domain FBD of the universal filter, the sinh-domain lossless integrator and summation/subtraction blocks are required and are thus presented in the following section.

2.1. Sinh-domain building blocks

The main building block for designing sinh-domain integrators is the nonlinear transconductor given in Figure 2a [5]. Utilizing the translinear principle and performing a routine algebraic analysis, it can be easily obtained that the output current is given by the following equation as:

$$i_{out} = 2I_o.\sinh\left(\frac{\hat{v}_{IN}}{U_T}\right). \tag{10}$$

This cell will be mentioned in the following as the $S+$ cell, while the corresponding notation is given in Figure 2b. The corresponding cell with an inverted output is shown in Figure 2c and it will be denoted as the $S-$ cell, as is depicted in Figure 2d. The SINH $^{-1}$ and SINH operators introduced in Eqs. (1) and (2), respectively, can be obtained from Figure 2a, as shown in Figures 3a and 3b, respectively [15].

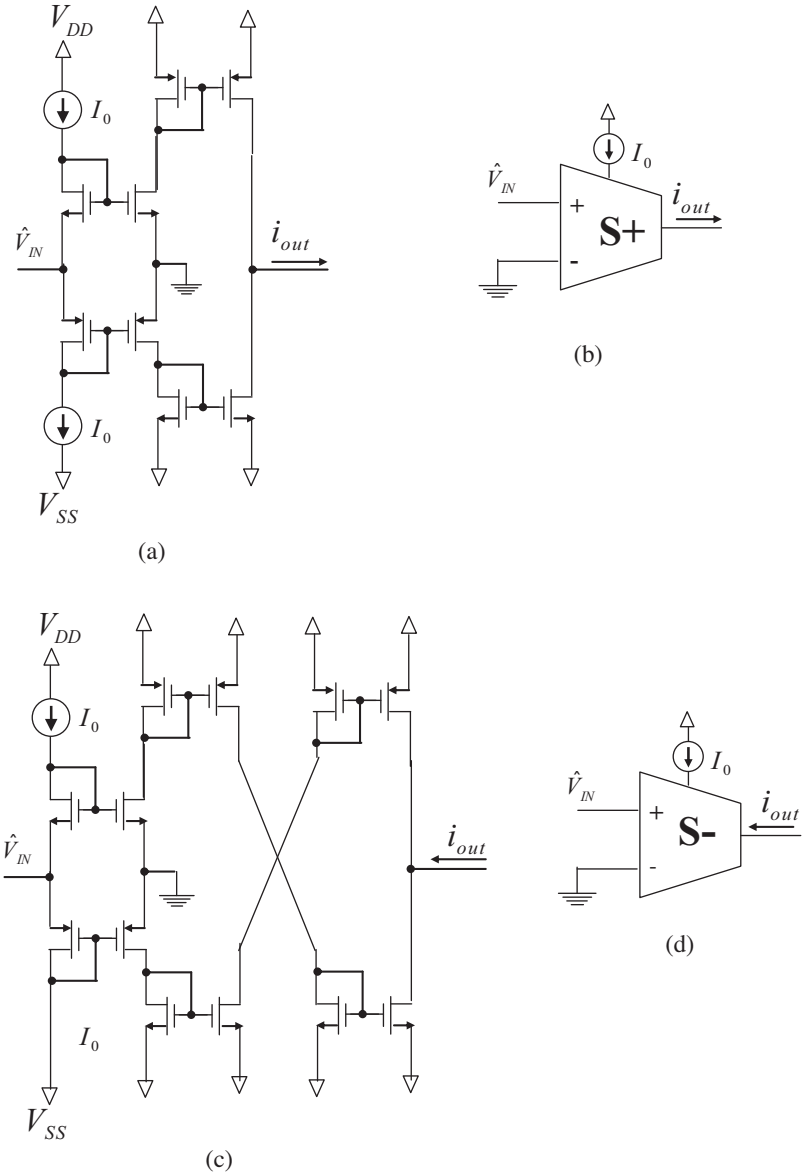

Figure 2. Sinh transconductors: a) positive transconductor, b) notation of the positive transconductor cell, c) negative transconductor, and d) notation of the negative transconductor cell [15].

Another important nonlinear transconductor block is that given in Figure 4a. The output current is given by the following equation as:

$$i_{out} = 2I_o . \cosh\left(\frac{\hat{v}_{IN}}{U_T}\right). \tag{11}$$

Thus, due to the hyperbolic cosine output-input relationship, this cell will be denoted as the $C+$ cell, as is shown in Figure 4b.

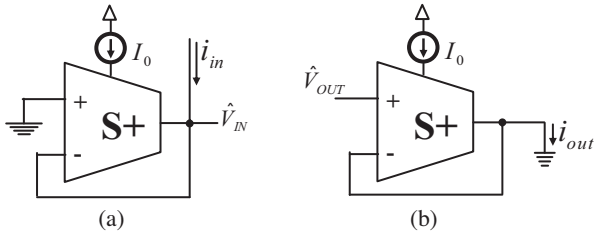

Figure 3. Realization of the operators: a) SINH $^{-1}$ and b) SINH [15].

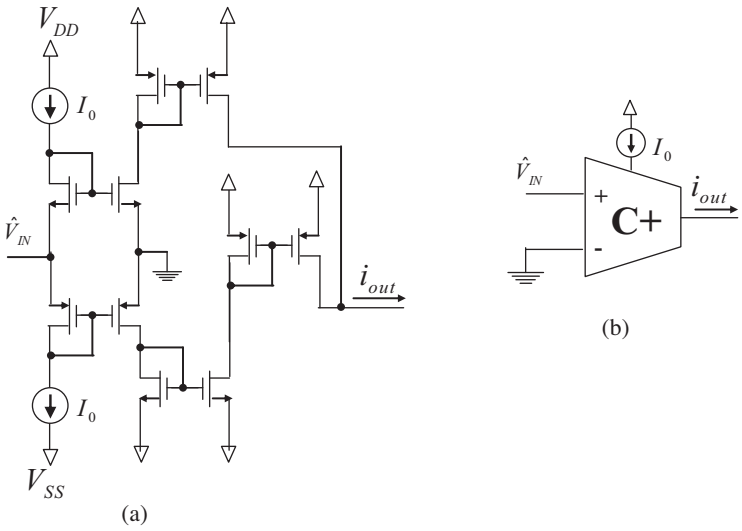

Figure 4. Cosh transconductor: a) positive transconductor, and b) notation of the positive transconductor cell [15].

The transconductor in Figure 4a is derived from the transconductor in Figure 2a by performing appropriate inversion of the intermediate signals.

Another important block that is required for realizing sinh-domain integrators is the 2-quadrant multiplier/divider block. A conceptual diagram of a 2-quadrant class-AB multiplier/divider block is that depicted in Figure 5a, whereas in Figure 5b, the notation of this block is given. It is constructed from 2 single-quadrant multipliers [12] and an appropriate splitter of the current i_1 in order to achieve a 2-quadrant operation. The realization of the multiplier is that shown in Figure 5c. The single-quadrant multipliers are constructed from transistors $M_{n1}-M_{n4}$ and $M_{p1}-M_{p4}$, respectively. The translinear loop formed by transistors $M_{n5}-M_{n6}$ and $M_{p5}-M_{p6}$ establishes that the outputs of the splitter are given by the expressions $i_{1p}=\left(i_1+\sqrt{i_1^2+4i_0^2}\right)/2$ and $i_{1n}=\left(-i_1+\sqrt{i_1^2+4i_0^2}\right)/2$. Taking also into account the condition $i_{1p}-i_{1n}=i_1$, it can be easily obtained that the output current is given by the following equation as:

$$i_{out}=I_o.\frac{i_1}{i_2}. \tag{12}$$

Using the building blocks presented in this section, the topologies of the corresponding sinh-domain integrators will be presented in the following.

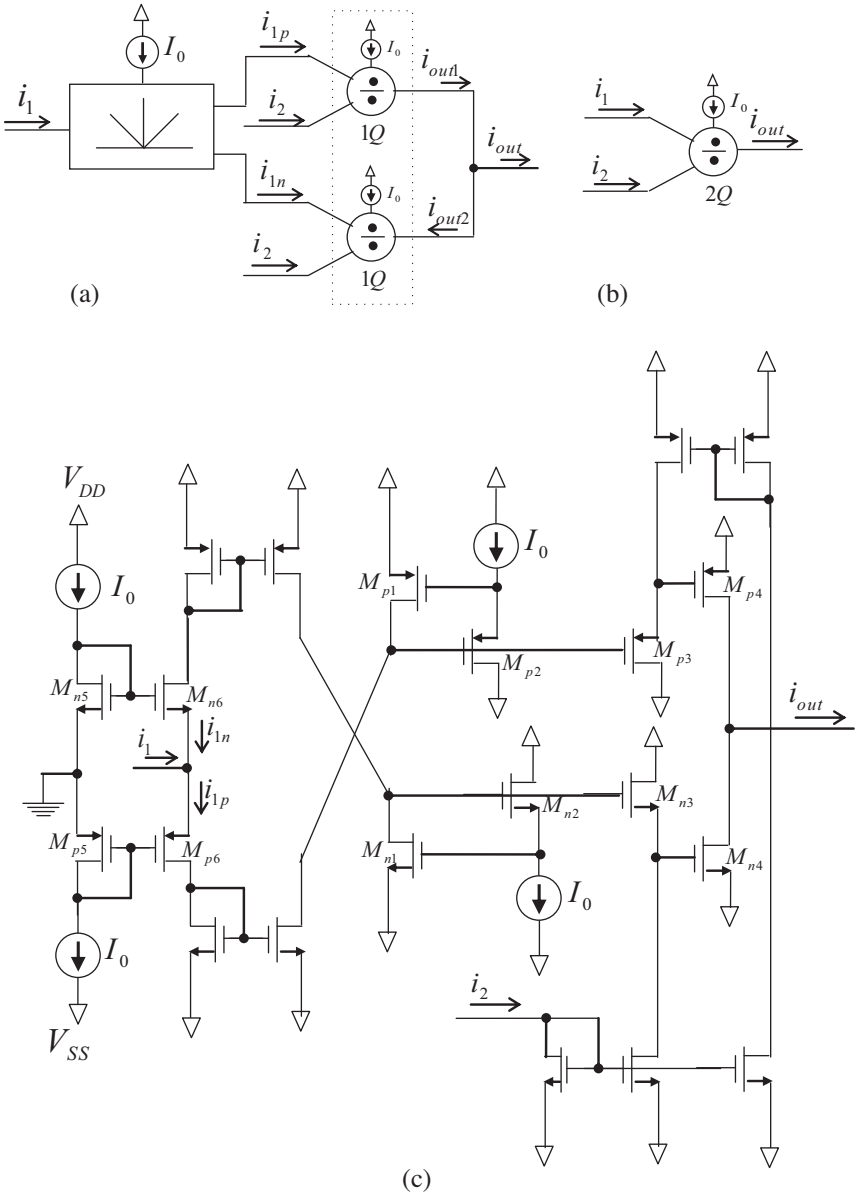

Figure 5. Two-quadrant multiplier: a) conceptual representation, b) notation, and c) topology [15].

2.2. Sinh-domain integrators

Let us consider a system that implements the transfer function of a lossless integrator $H(s) = 1/\tau s$. The expression that would be fulfilled by the corresponding nonlinear voltages is given by the following equation:

$$\hat{\tau}.\frac{d}{dt}SINH(\hat{v}_{OUT}) = SINH(\hat{v}_{IN}), \tag{13}$$

where $\hat{\tau}$ is the time constant in the sinh-domain.

Using the definition of the SINH operator described by Eq. (2) and considering that $\hat{\tau} = CU_T/2I_o$, the current that flows through the integration capacitor is given by the following equation as:

$$i_C = 2I_o.\frac{\sinh\left(\frac{\hat{v}_{IN}}{U_T}\right)}{\cosh\left(\frac{\hat{v}_{OUT}}{U_T}\right)} \quad . \tag{14}$$

The realization of the above expression is achieved by the topology in Figure 6. Figure 6 is the complete circuit of the current-mode lossless integrator, which includes the sinh-domain core and SINH and SINH $^{-1}$ blocks that realize the complementary operators.

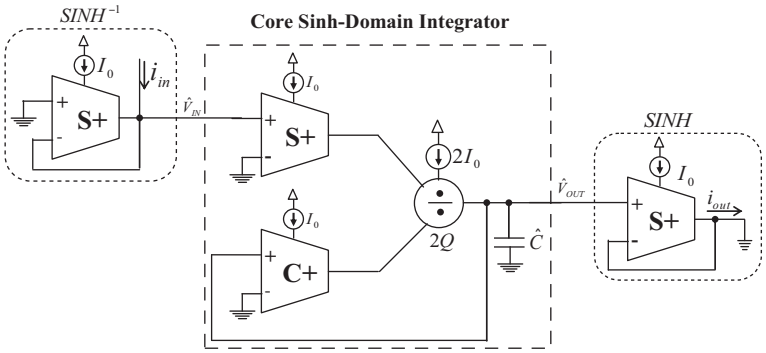

Figure 6. Complete linear sinh-domain lossless integrator.

2.3. Sinh-domain summation/subtraction block

The multiple-input algebraic summation block required for obtaining the proposed universal biquadratic filter is demonstrated in Figure 7. The expression for the output voltage is obtained as follows:

$$SINH\left(\hat{v}_{OUT}\right) = SINH\left(\hat{v}_{IN(0)}\right) \pm K_1.SINH\left(\hat{v}_{IN(1)}\right) \pm K_2.SINH\left(\hat{v}_{IN(2)}\right). \tag{15}$$

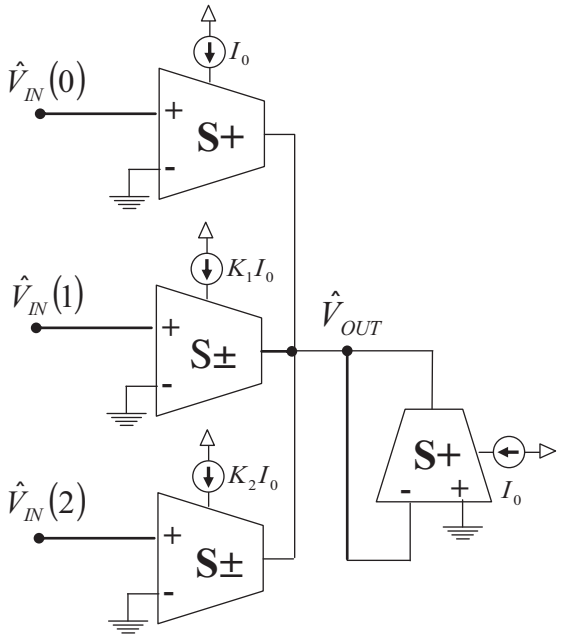

Figure 7. Sinh-domain multiple-input algebraic summation/subtraction block with weighted input.

3. Simulation results

In order to confirm the validity of our design, a sinh-domain counterpart of the universal biquadratic filter in Figure 1, using the building blocks mentioned in Section 3, was designed and the derived sinh-domain universal biquadratic filter is depicted in Figure 8.

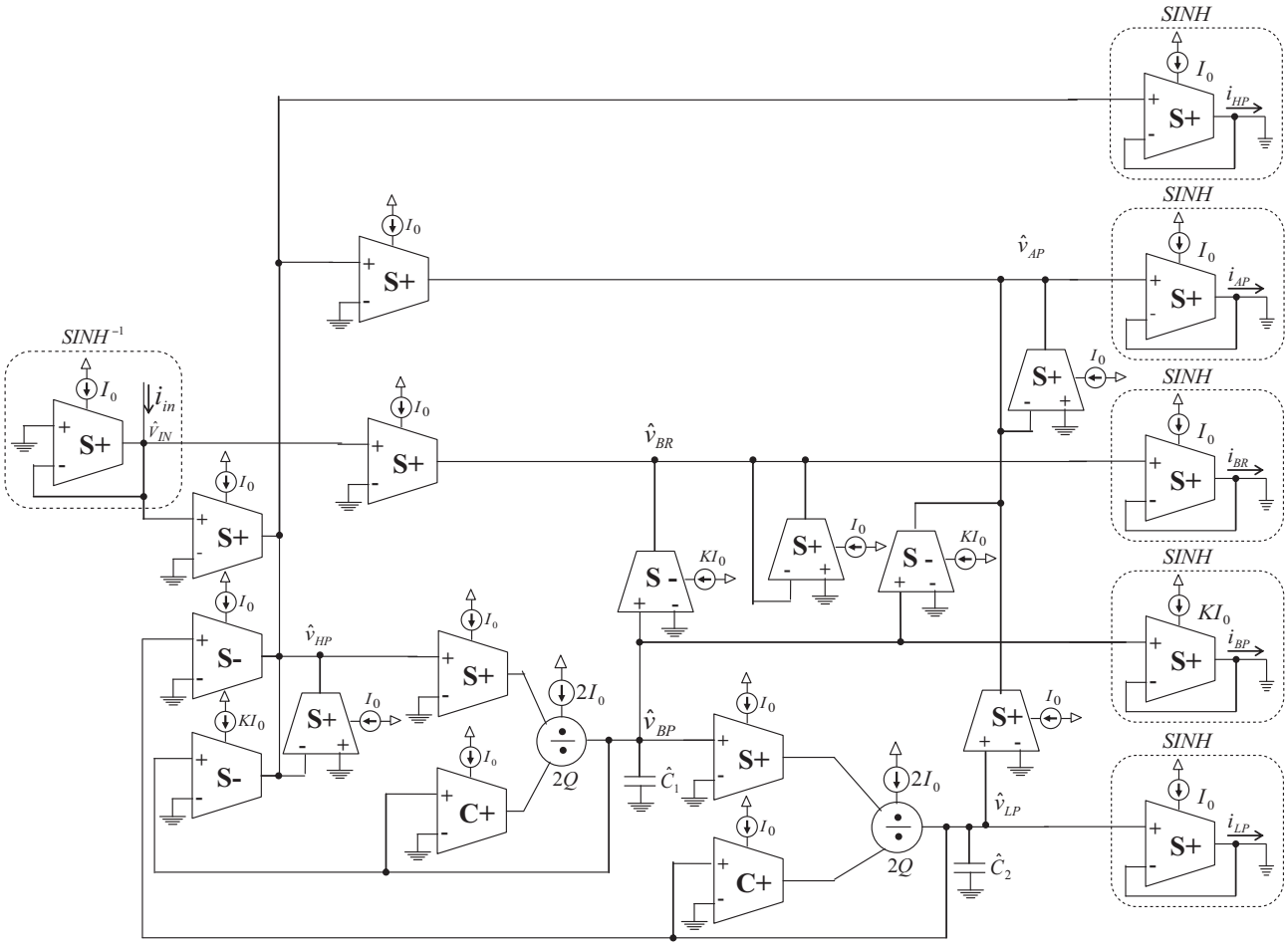

Figure 8. Topology of the proposed sinh-domain universal biquadratic filter.

The evaluation of the performance of the filters was done using Cadence Software. In addition, transistor models with the technology parameters provided by the Taiwan Semiconductor Manufacturing Company 0.18-μm complementary metal oxide semiconductor (CMOS) process were employed in the simulations. The aspect ratio of both the n-channel MOS (NMOS) and p-channel MOS (PMOS) transistors that construct the translinear loops in the S and C cells was chosen to be 8/8 μm, whereas the aspect ratios of the other NMOS and PMOS transistors were 8/8 μm and 80/8 μm, respectively. A symmetrical supply voltage equal to ± 0.75 V was chosen, while the DC current I_0 was 100 pA. The DC power dissipation for the filter was 19.2 nW. The frequency response with a cut-off frequency f_0 = 13 Hz, which is typical for an EEG application, was realized.

Considering that n = 1.32 and $\hat{\tau} = CU_T/2I_o$, for the above value of the cut-off frequency, the value of the capacitors was chosen as 75.3 pF. The simulated magnitude response of the sinh-domain universal biquadratic filter is therefore given in Figure 9. Figure 10 shows the phase response of the AP output. Figure 11 shows the

time-domain response of the AP output. A sine-wave input at a frequency of 13 Hz with a modulation index factor m = 50% was applied to the filter. This causes a 38.16 ms time delay in the AP output, corresponding to a 178.60 phase difference, which is close to the theoretical value (180°).

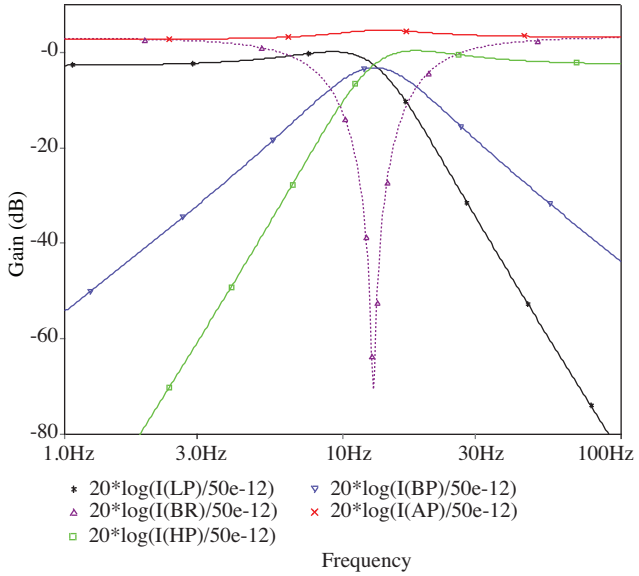

Figure 9. Simulated frequency responses of the proposed universal biquadratic filter in Figure 8.

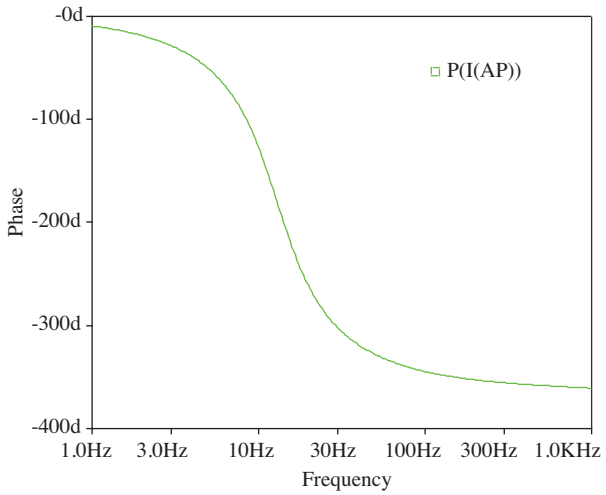

Figure 10. Phase response of the AP output of the proposed sinh-domain universal biquadratic filter.

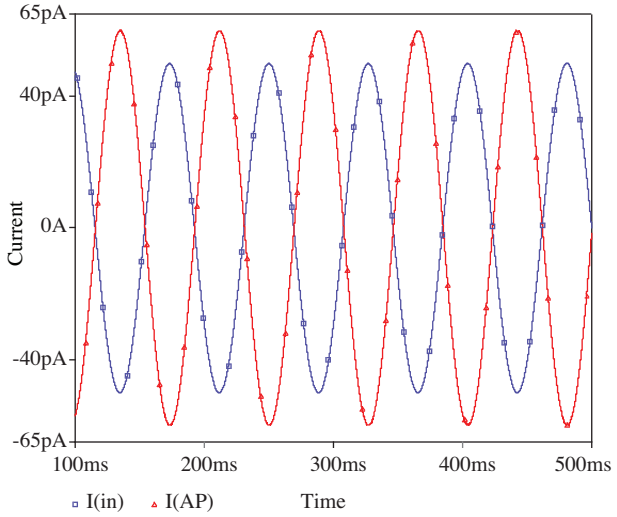

Figure 11. Time-domain responses of the AP output of the proposed sinh-domain universal biquadratic filter.

The electronic tunability of the proposed sinh-domain universal biquadratic filter topology, concerning its frequency characteristics, is demonstrated by performing simulations of its frequency response at different levels of current I_0. The derived responses for f_0 = 5 Hz, 13 Hz, and 35 Hz are simultaneously plotted in Figure 12, where the capability for the electronic tuning of the proposed sinh-domain universal biquadratic filter can be verified. For the above values of the frequencies, I_0 was varied from 38.4 pA to 269.2 pA. The feature for the orthogonal adjustment between the resonant frequency and the Q factor offered by the proposed filter

has been verified through the plot depicted in Figure 13. In Figure 13, the BP filter responses, obtained for K = 0.33, 0.5, and 1, are demonstrated. According to Eq. (9), the theoretically predicted values of Q are 3, 2, and 1. The obtained values from the plot in Figure 13 were 2.88, 1.92, and 0.95, respectively. Due to the fact that the center frequency of the BP filters remains unaffected during the tuning of Q, it is obvious that this is an orthogonal procedure with regards to the tuning of ω_0.

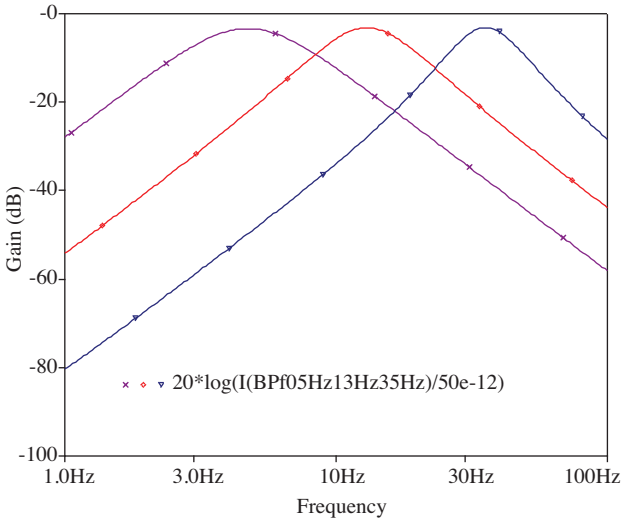

Figure 12. Demonstration of the electronic tunability of frequency characteristics.

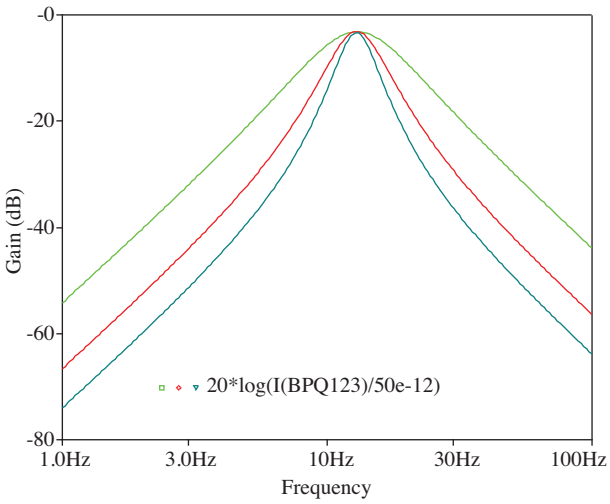

Figure 13. Demonstration of the independent tunability pole frequency (ω_0) and the quality factor (Q).

The total harmonic distortion (THD) analysis usually considered for deriving distortion analysis is not appropriate. By applying an input signal close to the fundamental frequency at the input of a filter, the corresponding harmonics usually fall into the stop-band, and thus an underestimation of the nonlinearity at the output of the filter will be achieved. The problem is usually prominent in the case of BP responses. Thus, a more practical way for evaluating the nonlinear performance is to perform the well-known third-order intermodulation distortion (IMD3) test. Therefore, to study the nonlinear behavior of the proposed sinh-domain universal biquadratic filter topology, the IMD3 (for the BP response) test was employed. Accordingly, 2 closely spaced tones, 11 and 12 Hz, which fall into the pass-band of the BP response, were applied at the input of the filter. The simulated IMD3 versus the modulation index factor is plotted in Figure 14. The simulated root mean square (RMS) value of the input signal amplitude for a 1% distortion level was 60.9 pA.

Integrating the noise over a 50 Hz range, the calculated RMS value of the noise was 0.067 pA. The signal-to-noise ratio (SNR) versus modulation index factor is plotted in Figure 15. The predicted dynamic range (DR), at a distortion level of 1%, would be equal to 59.17 dB.

The proposed biquadratic filter was designed using the log- and square root-domain techniques, as well as the OTA derived according to [21]. The performance of the proposed sinh-domain biquadratic filter was compared with those of the corresponding log-domain, square root-domain, and OTA-based designs.

An estimation of the power efficiency of the filters is given by utilizing the figure of merit (FOM) given by Eq. (16):

$$FOM = \frac{P}{n \cdot f_o \cdot (DR)}, \tag{16}$$

where P is the power dissipation of the filter, n is the number of poles, f_o is the cut-off frequency, and DR is the dynamic range.

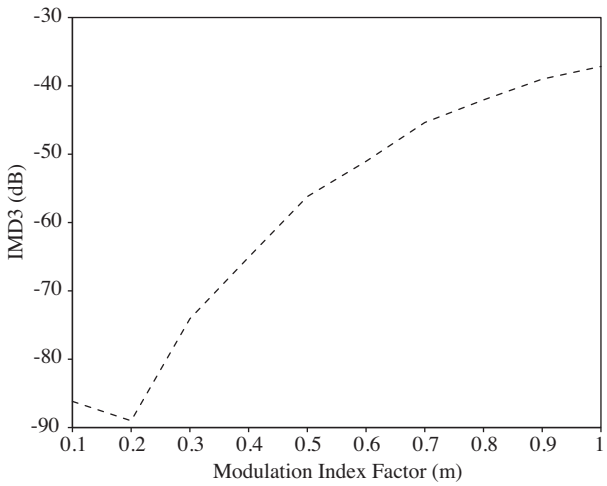

Figure 14. Nonlinear performance of the proposed sinh-domain universal biquadratic filter.

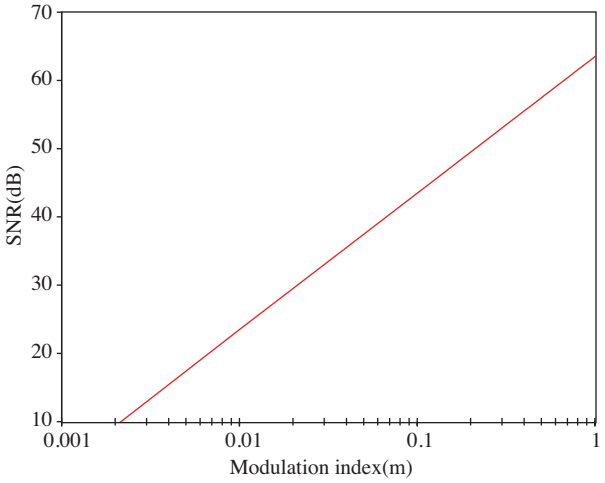

Figure 15. Simulated SNR versus modulation index factor.

The derived results are summarized in the Table, where it can readily be seen that the proposed sinh-domain biquadratic filter offers a more power efficient design, better sensitivity performance, and less capacitance than that of the corresponding log-domain techniques, square root-domain techniques, and OTA-based designs. Moreover, and more importantly, it has low bias and power dissipation values.

Table. Performance comparison results for the proposed sinh-domain biquadratic filter.

Performance factor	Log-domain design	Square root-domain design	OTA design [21]	Proposed
Power supply voltage	1.5 V	1.5 V	0.75 V	0.75 V
Bias current	25 μA	5 μA	5n A	100 pA
Power dissipation	3.46 mW	209 uW	424 nW	19.2 nW
Total capacitance (pF)	24.5 uF	643 nF	1.71 nF	150.6 pF
RMS ampl. @ THD level 1%	13.6 uA	2.62 uA	72.1 mV	60.9 pA
RMS value of output noise	33.6 nA	7.13 nA	346.9 uV	0.067 pA
Dynamic range	52.14 dB	51.3 dB	46.35 dB	59.17 dB
Std. dev. of mid-freq. gain	1.7086 m	202.3774 u	474.3 u	392.7014 u
Std. dev. of center freq. f_o	269.89 m	286.4307 m	324.7 m	274.69 m
FOM	329 nJ	21.9 nJ	78.5 pJ	0.813 pJ

4. Conclusion

The design procedure for deriving a low-voltage sinh-domain universal biquadratic filter for neuromorphic systems and biomedical applications is well facilitated by employing the proposed sinh-domain topology constructed from lossless integrators. Among the offered benefits, the most important are low-power consumption and the capability for electronic tuning of the resonant frequency of the filter and independent adjustment of pole frequency (ω_0) and the quality factor (Q) under a low-voltage environment. The proposed topology is free from matching conditions, capable of absorbing the shunt parasitic capacitances, amenable for monolithic integra-

tion, and composed of merely a few transconductor cells and grounded elements, and thus it could be used for realizing low-voltage, low-frequency analog processing systems.

Acknowledgments

The authors would like to thank the anonymous reviewers for their constructive comments and suggestions. The authors would also like to thank the Office of the University Grants Commission, Government of India, India, for supporting this work under the major research project scheme.

References

[1] C. Tomazou, F.J. Lidgey, D.G. Haigh, Analogue IC Design: The Current-Mode Approach, London, UK, Peregrinus, 1990.

[2] J. Ramirez-Angulo, M. Robinson, S. Sinencio, "Current-mode continuous-time filters: two design approaches", IEEE Transactions on Circuits and Systems, Vol. 39, pp. 337–341, 1992.

[3] Y. Tsividis, V. Gopinathan, L. Toth, "Companding in signal processing", Electronics Letters, Vol. 26, pp. 1331–1332, 1990.

[4] Y. Tsividis, "On linear integrators and differentiators using instantaneous companding", IEEE Transactions on Circuits and Systems II, Vol. 42, pp. 561–564, 1995.

[5] D. Frey, "Exponential state-space filters: a generic current mode design strategy", IEEE Transactions on Circuits and Systems I, Vol. 43, pp. 34–42, 1996.

[6] A.L. Martin, A. Carlosena, "Synthesis of sinh systems from Gm-C systems by component to component substitution", Proceedings of the 42nd Midwest Symposium on Circuits and Systems, pp. 287–290, 1999.

[7] W. Serdijn, M. Kouwenhoven, J. Mulder, A. van Roermund, "Design of high dynamic range fully integratable translinear filters", Analog Integrated Circuits and Signal Processing, Vol. 19, pp. 223–239, 1999.

[8] A. Katsiamis, K. Glaros, E. Drakakis, "Insights and advances on the design of CMOS sinh companding filters", IEEE Transactions on Circuits and Systems I, Vol. 55, pp. 2539–2550, 2008.

[9] J.L. Andreassi, Psychophysiology: Human Behavior and Physiological Response, 5th ed, Mahwah, NJ, USA, Lawrence Erlbaum Associates, 2007.

[10] S.S. Bustos, J.S. Martínez, F. Maloberti, E.S. Sinencio, "A 60-dB dynamic-range CMOS sixth-order 2.4-Hz low-pass filter for medical applications", IEEE Transactions on Circuits and Systems II, Vol. 47, pp. 1391–1398, 2000.

[11] D. Frey, A. Tola, "A state-space formulation for externally linear class AB dynamical circuits", IEEE Transactions on Circuits and Systems II, Vol. 46, pp. 306–314, 1999.

[12] P. Poort, W. Serdijn, J. Mulder, A. van der Woerd, "A 1-V class AB translinear integrator for filters applications", Analog Integrated Circuits and Signal Processing, Vol. 21, pp. 79–90, 1999.

[13] S. Haddad, W. Serdijn, "An ultra low-power class-AB *Sinh* integrator", Proceedings of the 19th Annual Symposium on Integrated Circuits and Systems Design, pp. 74–79, 2006.

[14] T. Halvorsrød, W. Luzi, "A low power, extended dynamic range, fully differential, class AB, log-domain allpass filter", NorChip, Riga, 2003.

[15] C. Kasimis, C. Psychalinos, "Design of sinh-domain filters using complementary operators", International Journal of Circuit Theory and Applications, Vol. 40, pp. 1019–1039, 2011.

[16] L.D. Paarmann, Design and Analysis of Analog Filters - A Signal Processing Perspective, Dordrecht, Kluwer Academic Publishers, 2001.

[17] L.S.Y. Wong, S. Hossain, A.T.J. Edvinsson, D.H. Rivas, H. Naas, "A very low-power CMOS mixed-signal IC for implantable pacemaker applications", IEEE Journal of Solid-State Circuits, Vol. 39, pp. 2446–2456, 2004.

[18] S.S. Bustos, J.S. Martínez, F. Maloberti, E.S. Sinencio, "A 60-dB dynamic-range CMOS sixth-order 2.4-Hz low-pass filter for medical applications", IEEE Transactions on Circuits and Systems II, Vol. 47, pp. 1391–1398, 2000.

[19] A. van Schaik, S.C. Liu, "AER EAR: a matched silicon cochlea pair with address event representation interface", IEEE International Symposium on Circuits and Systems, Vol. 5, pp. 4213–4216, 2005.

[20] G. Indiveri, E. Chicca, R. Douglas, "A VLSI array of low-power spiking neurons and bistable synapses with spike-timing dependent plasticity", IEEE Transactions on Neural Networks, Vol. 17, pp. 211–221, 2006.

[21] E.D.C. Cotrim, L.H. de Carvalho Ferreira, "An ultra-low-power CMOS symmetrical OTA for low-frequency Gm-C applications", Analog Integrated Circuits and Signal Processing, Vol. 71, pp. 275–282, 2012.